Numerical Investigation of The Performance of Fully Solar Driven Compact HDH Desalination System

Khaled Alshamrani *khaled.s.m.alshamrani@gmail.com*
Faculty of Engineering / Mechanical Engineering Department *391001652@stu.ut.edu.sa*
University of Tabuk
Tabuk 47913, Saudi Arabia

Ahmed Asiri *asiriahm7@gmail.com*
Faculty of Engineering / Mechanical Engineering Department *391002549@stu.ut.edu.sa*
University of Tabuk
Tabuk 47913, Saudi Arabia

Ali Alqarni *eng.alialqarni@icloud.com*
Faculty of Engineering / Mechanical Engineering Department *391003758@stu.ut.edu.sa*
University of Tabuk
Tabuk 47913, Saudi Arabia

Hossam AbdelMeguid *habdelmeguid@ut.edu.sa*
Faculty of Engineering / Mechanical Engineering Department
University of Tabuk
Tabuk 47913, Saudi Arabia

Abstract

Climate change is characterized by long-term changes in weather patterns and temperatures, which may occur naturally through solar cycle variations. However, human activities, particularly the burning of fossil fuels like coal, oil, and gas, have been the primary cause of climate change since the 1800s. Global climate change affects water resources through increased evaporation rates, decreased water quality in inland and coastal areas, higher water temperatures, earlier and shorter runoff seasons. These effects have significant implications for water availability and management. This paper provides an overview of the different methods of desalination and focuses on the use of a compact and domestic air humidification dehumidification (HDH) desalination system, which is suitable for remote areas with limited water resources and experienced operators. The study presents a mathematical model to analyze the impact of various operating parameters on the system's productivity. The mathematical model is solved using a MATLAB, and a series of numerical runs are performed under different operating and design parameters. The study presents the transient state behavior of the system and its productivity. Overall, the report provides valuable insights into the use of HDH desalination systems in remote areas and highlights the importance of both theoretical and experimental investigations in improving the efficiency of such systems.

Keywords: HDH, Solar Desalination, Decentralized Desalination.

1. INTRODUCTION

Water resources are essential for both human society and ecosystems, as we rely on a clean and reliable supply of water for various purposes such as drinking, agriculture, energy production, and recreation. Without water, life on Earth is not possible. Therefore, it is important to save clean water for future generations and the wellness of wildlife animals. Unfortunately, many regions suffer from water scarcity or lack of water.

In the Gulf countries, the lack of river water and limited seasonal valleys have prompted the expansion of desalination to meet the increasing demand for water, despite its high cost. Saudi

Arabia depends on groundwater, desalinated sea water, recycled water, and surface water sources for obtaining water. NEOM, a new city being built in Saudi Arabia, will rely on sustainable, carbon-free technologies powered by 100% renewable energy to desalinate water and recycle wastewater for irrigation and other purposes. NEOM aims to recover all resources from wastewater for use in energy, construction, agriculture, and landscaping through the use of integrated seawater resource recovery treatment.

Seawater desalinationis a potential solution for increasing water resources in the long term, especially if renewable energy sources such as solar, wind, and nuclear power are utilized. Additionally, rationalizing water consumption can help to conserve this valuable resource. Although desalination is more energy-intensive than other sources of fresh water, it is a valuable option in areas like the Gulf countries where water scarcity is a major issue.

Reverse osmosis (RO) is a process of desalination that separates the saline feedwater into low-salinity product water and very saline concentrate streams. RO systems have four major components: pretreatment, pressurization, membrane separation, and post-treatment stabilization. The product water produced by the process is suitable for most domestic, industrial, and agricultural uses, while the by-product of brine is a concentrated salt solution that must be carefully disposed of. The advantages of RO include its simplicity, low installation cost, and low environmental impact. However, RO membranes are sensitive to abuse and require high-quality materials and equipment. Additionally, the feedwater must be pretreated, and there is a risk of bacterial contamination.

Thermal desalination processes include Single Effect Evaporation and Multistage Flash Desalination (MSF). Single Effect Evaporation has limited industrial use and is mostly used in marine vessels because the amount of water produced is less than the amount of heating steam used to operate the system. Multistage Flash Desalination is a widely used process that distills seawater by flashing a portion of the water into steam in multiple stages of heat exchangers. MSF plants produce about 26% of all desalinated water in the world, but new plants are using reverse osmosis due to lower energy consumption. MSF configurations include Once Through MSF and MSF with brine circulation, which improve system performance ratio and thermal efficiency.

Solar distillation is a process that replicates the natural water cycle by heating sea water through the sun's energy causing evaporation, and then the water vapor is condensed onto a cool surface. There are two types of solar distillation, one that uses photovoltaic cells to convert solar energy to electrical energy to power desalination and the other one, known as solar thermal powered distillation, converts solar energy to heat. Solar stills are used to distill water with substances dissolved in it, purifying it by using the heat of the Sun to evaporate water so that it may be cooled and collected. The process eliminates impurities and microbiological organisms, resulting in pure, potable water.

2. LITERATURE REVIEW

The challenges associated with developing new communities are particularly related to the shortage of natural resources such as water and clean energy. To meet the requirements of these communities, renewable energy sources such as wind, wave, tidal, and solar energy must be utilized, as indicated in various studies (R Farmani et al., 2011; Raziyeh Farmani et al., 2012; Memon et al., 2011; Ward et al., 2011). Solar energy, in particular, appears to be a promising solution, given its availability in the Middle East and North Africa, especially in the Arabian Peninsula, and its diverse applications, including solar cooling (I. I. El-Sharkawy et al., 2013; Ibrahim I. El-Sharkawy et al., 2014; Ibrahim I El-Sharkawy et al., 2013), solar heating (Abu Mallouh et al., 2022), green hydrogen production (Nakamura et al., 2015; Sukpancharoen & Phetyim, 2021), desalination (Elsharkawy et al., 2014; Kabeel et al., 2022a, 2022b), and electrical energy generation.Humidification-dehumidification (HDH) is a thermal desalination process that uses a humidifier, a dehumidifier, and a heater to imitate the natural rain cycle. In the humidifier, salty water humidifies air, and in the dehumidifier, hot moist air comes in contact with cold salty water, causing water vapor to condense, creating fresh water. There are various configurations of

the HDH system that can be used, and their effectiveness can be measured using exchanger effectiveness and efficiency.

2.1 History and Background

The history and background of humidification-dehumidification (HDH) desalination dates back to ancient times when people used the sun and natural materials to distill water. However, the modern development of HDH desalination began in the 1950s and 1960s when researchers began experimenting with thermal desalination methods. In the early 1970s, HDH was developed as a new technology that uses low-temperature heat sources to produce fresh water (Manju & Sagar, 2017). The process is based on the principle of humidification and dehumidification, mimicking the natural water cycle. Since then, the technology has been studied and developed by researchers worldwide, and it is now considered a promising and efficient method for small to medium scale desalination applications, particularly in remote areas.Since then, HDH desalination systems have been developed and implemented on a larger scale, mainly in coastal regions where seawater is abundant but freshwater resources are scarce, such as in the Middle East and North Africa. HDH has been used in many countries, including Saudi Arabia, United Arab Emirates, Kuwait, Bahrain, and Oman, to provide drinking water and water for agricultural purposes (Sayed et al., 2022). HDH desalination offers several advantages over other desalination methods. The process is simple, reliable, and requires minimal maintenance. The system is also cost-effective, and the use of renewable energy sources such as solar, wind, and geothermal energy can make the system more sustainable.Despite its advantages, HDH is not without its limitations. One major challenge is the high energy consumption required to produce water. The process also produces a significant amount of brine, which can pose an environmental challenge if not disposed of properly (Tahir & Al-Ghamdi, 2022). In summary, HDH desalination is a method that has been in use for thousands of years and continues to be researched and developed today. Despite its limitations, HDH offers a simple, reliable, and cost-effective way to provide drinking water and water for agricultural purposes to regions with limited access to fresh water.

2.2 Solar Powered HDH Desalination

Solar-powered Humidification-Dehumidification (HDH) desalination is an advancement of the traditional HDH process that harnesses renewable energy sources to operate. The history of solar-powered HDH is closely intertwined with that of HDH itself. The exploration of solar energy as a heat source for the HDH process began in the 1970s, as researchers recognized its potential for powering the desalination process. The HDH process requires low-temperature heat, making it suitable for utilizing solar energy. While HDH has been used in remote areas on a small scale for decades, its large-scale application was hindered by high costs until the use of solar energy as a primary energy source became feasible. One of the earliest large-scale solar-powered HDH projects was initiated in Riyadh, Saudi Arabia in the early 1980s, which used solar energy to generate heat for the process. Several pilot-scale and commercial-scale solar-powered HDH desalination systems have since been developed in the Middle East and North Africa, where solar energy is abundant, to provide freshwater in remote areas without grid power. Nowadays, solar-powered HDH desalination is being developed globally, especially in regions with scarce freshwater and abundant renewable energy sources like solar. The implementation of solar-powered HDH systems offers many benefits such as increased flexibility, reduced operating costs, and lower environmental impact. To summarize, solar-powered HDH desalination is a recent development in the HDH process that takes advantage of renewable energy sources to provide a cost-effective and eco-friendly solution for producing freshwater in remote and arid regions.

One possible application for sustainable water supply is solar desalination of seawater, which can be accomplished using solar energy, providing a sustainable source of freshwater. Several solar-powered desalination technologies exist, including thermal-driven membrane (TDM) (Criscuoli & Carnevale, 2022; Shafieian et al., 2020a, 2020b; Zaragoza et al., 2014), humidification and dehumidification (HDH) (Abdel Dayem & AlZahrani, 2022; Elzayed et al., 2021; Khalaf-Allah et al., 2022; A. S. A. Mohamed et al., 2021), and solar stills (SS) (Abdullah et al., 2021; Ahmed et

al., 2021; Mohaisen et al., 2021; Prakash & Jayaprakash, 2021). The subsequent sections of this paper present the contributions made in modeling, optimizing, developing, and enhancing the performance of HDH desalination.

In a study by (A. M. I. Mohamed & Elminshawy, 2009), a sea water desalination system powered by geothermal energy was evaluated. The study indicated that geothermal energy could effectively power the system, and by optimizing the ratio of sea water mass flow rate to air mass flow rate, geothermal source inlet temperature, and cooling water temperature difference across the condenser, the freshwater productivity could be improved.

(Kabeel et al., 2013) investigated a proposed desalination system based on air humidification-dehumidification and its theoretical and experimental performance. They developed a simulation model to assess the productivity of the system at different operating times during the day and found that the highest freshwater productivity occurred during the second operating period. The study validated the theoretical results with experimental results, which showed good agreement, and the model was deemed valid under various boundary conditions. The system operating for four hours a day with preheating showed the highest productivity, producing about 22 L/day, and the estimated total cost per 1 L of the unit was 0.0578$. The study concluded that the proposed mathematical model could simulate the heat exchange accurately, calculate the system temperatures at steady state conditions, and determine the best operating time during the day. Additionally, the study found that the unit productivity increased as the water temperature entering the humidifier increased and that the proposed model was reliable in predicting the unit's performance under different boundary conditions.

(El-Ghetany & Khattab, 2016) conducted a theoretical analysis of a water desalination system that utilized a humidification-dehumidification process enhanced with solar energy. The study found that the system was feasible and had good potential in rural coastal areas that require a sustainable supply of fresh water. The daily production of condensed water was influenced by factors such as saline water flow rate, temperature, air mass flow rate, and pressure, and increasing the ambient air flow rate resulted in a decrease in the amount of water vapor inside the atomization chamber.

A study by (Aburub et al., 2017) experimentally investigated the performance of a water-heated humidification-dehumidification desalination system with brine recirculation and studied the effect of the mass ratio and hot water temperature on the system's Gain Output Ratio (GOR), Recovery Ratio (RR), humidifier, and dehumidifier effectiveness. The study found that the system could produce around 92 liters of distillate water per day, with a GOR of 1.3 and the components' effectiveness ranging from 92-97% and 53-79% for the dehumidifier and humidifier, respectively.

(Moumouh et al., 2018) investigated a modular humidification-dehumidification water desalination system consisting of a water heater, an evaporator, and a condenser. They conducted experimental studies to analyze the effect of air and water temperature, as well as the mass flow rates of air and water, on freshwater productivity. The results revealed an optimal mass flow rate ratio that resulted in maximum freshwater productivity.

In their research, (Fares et al., 2019) proposed a novel water desalination system that aims to minimize power consumption. The system combines thermal pump, wetting technology, and dehumidification while controlling water and air flow rates. The system is portable, operates at low temperature, and has a small size. The system achieved a maximum freshwater productivity of 1.14 kg/hr with minimum power consumption of only 1839 kJ/kg. The maximum GOR value was 1.34 achieved at water and air flow rates of 15 and 100 kg/hr, respectively, and the maximum COP value was 3.6 achieved at flow rates of water and air of 18 and 134 kg/hr, respectively. These results are important in reducing energy consumption in small-scale desalination units."

2.3 Problem Statement

the scarcity of sustainable and renewable sources of water in Saudi Arabia is due to low rainfall. The issue impacts all sectors of development, including factories, businesses, and population

growth. Additional costs are incurred by these entities to obtain water supplies or extend their networks. To address this challenge, a potential solution is to explore a solar-powered humidification-dehumidification (HDH) desalination system as a source of water.

3. METHODOLOGY

The paper discusses the use of a mathematical model to analyze the impact of various operating parameters on the productivity of a compact and domestic air humidification dehumidification (HDH) desalination system. The mathematical model is solved using MATLAB, and a series of numerical runs are performed under different operating and design parameters. The study presents the transient state behavior of the system and its productivity. Therefore, the adopted methodology in terms of research design is a mathematical modeling approach. The data used in the mathematical model is obtained from previous studies and experiments. The data analysis is done using MATLAB to solve the mathematical model and perform numerical runs. The methodology used in this paper is deductive, as it starts with a theoretical framework and uses it to analyze the impact of various operating parameters on the productivity of the HDH desalination system.

4. SYSTEM DESCRIPTION

The solar powered HDH desalination system shown in FIGURE1 utilizes fixed PV panels and solar thermal collectors to operate. The system is divided into three main sections: PV panels, an evacuated tube solar water collector (SWC), and an HDH desalination unit. The required electricity to drive the air fan and pump is generated by two PV panels. These panels also pre-heat the seawater before it enters the evacuated solar collector and cool the panels to increase their conversion efficiency. The PV system contains charge controllers, batteries, and DC drives. Two parallel-connected evacuated tube SWCs are used to heat the seawater before it enters the humidifier of the HDH desalination unit, which comprises a humidifier and a dehumidifier. The rejected brine water is discharged from the humidifier and stored in the brine tank.

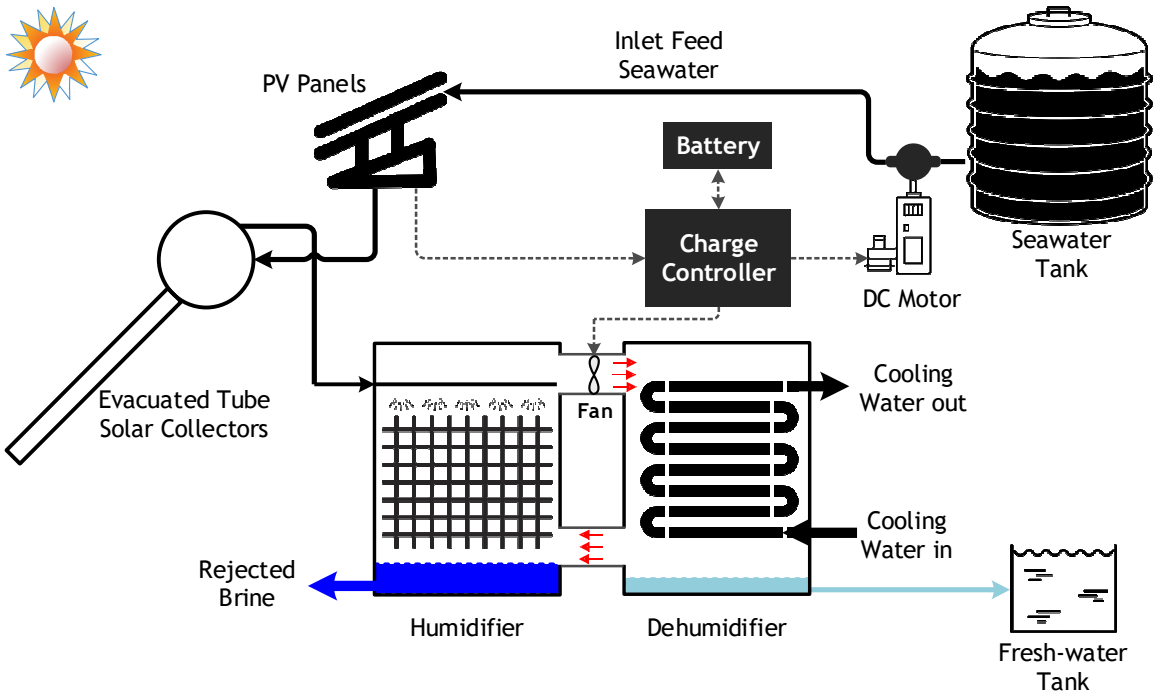

FIGURE1A: Schematic diagram of the proposed solar powered HDH desalination system.

5. MATHEMATICAL MODEL

To develop a steady-state mathematical model for an HDH (Humidification-Dehumidification) desalination system, the physical and thermodynamic processes within the system is analyzed and represented through mathematical equations. This involves applying the conservation equations of mass, energy, and momentum as the basis of the model. The system is divided into its components, including the T-PV, solar collectors, humidifier, dehumidifier, heat exchangers, pumps, and fans, with mathematical equations developed to describe each component's behavior. These equations take into account the physical and thermodynamic properties of the components, including heat transfer coefficients, pressure drops, and mass transfer rates. The mass and energy balances of each component are formulated based on their input and output flows, and the equations are solved simultaneously to obtain steady-state values for variables such as desalinated water temperature and concentration, air flow rate, and heat transfer rates. Using this model, the design and operation of the HDH system can be optimized and its performance predicted under different conditions, such as determining the optimal air flow rate, heat exchanger design, and operating temperatures for the humidifier and dehumidifier to maximize system efficiency. See the mathematical model below.

Equation	No.
$$T_{bs} = \frac{h_{p1}(\alpha\tau)_{eff} I(t) + U_{tT} T_a + h_T T_w}{U_{tT} + h_T}$$	1
$$T_c = \frac{\tau_G\left[\alpha_C \beta_C + \alpha_T (1-\beta_C)\right] I(t) - \eta_C I(t) \beta_C + U_t T_a + U_T T_{bs}}{U_t + U_T}$$	2
$$\eta_C = \eta_o\left[1 - 0.0045(T_C - 298.15)\right]$$	3
$$T_{sw2} = \left[\frac{h_{p1} h_{p2} (\alpha\tau)_{eff} I(t)}{U_L} + T_a\right]\left[1 - \exp\left(-\frac{F' A_C U_L}{m C_p}\right)\right] + T_{sw1} \exp\left(-\frac{F' A_C U_L}{m C_p}\right)$$	4
$$(\alpha\tau)_{eff} = \tau_G\{\beta_C + \alpha_T(1-\beta_C) - \eta_C \beta_C\}$$	5
$$U_L = U_{tw} + U_b$$	6
$$U_{tw} = \left[\frac{1}{U_{tT}} + \frac{1}{hi}\right]^{-1}$$	7
$$U_b = \left[\frac{L_i}{k_i} + \frac{1}{hi}\right]^{-1}$$	8
$$U_{tT} = \frac{(U_T \times h_T)}{(U_T + h_T)}$$	9
$$U_T = \left[\left(\frac{L_g}{k_g}\right) + \left(\frac{1}{h_{o(i)}}\right)\right]^{-1}$$	10
$$\dot{Q}_{total} = \dot{Q}_u + \dot{Q}_{loss} = D_{abs} \times L \times N \times a_{abs} \times \tau_g \times DNI$$	11
$$T_{SW,3} = T_{SW,2} + \frac{\dot{Q}_u}{\dot{m}_{sw} \times C_p} = T_{sw,2} + \frac{\dot{Q}_{total} - \dot{Q}_{loss}}{\dot{m}_{sw} \times C_P}$$	12
$$\dot{Q}_{loss} = \pi D_{abs} \times L \times N \times \left[h_{abs-g}(T_{abs} - T_a) + \sigma \varepsilon_{abs}\left(T_{abs}^4 - T_S^4\right)\right]$$	13
$$T_S = 0.05527 T_a^{\frac{3}{2}}$$	14
$$\varepsilon_{abs} = 0.062 + 2\times10^{-7}(T_{abs} - 273.15)^2$$	15
$$\dot{Q}_{total} = \dot{Q}_u + \dot{Q}_{lass} = A_c F_R(\alpha_p \tau_g) DNI$$	16

$\dot{Q}_{loss} = A_c F_R U_{loss} \left(T_{abs} - T_a\right)$	17
$\dot{Q}_u = \dot{m}_a C_{pa} \left(T_{a,2} - T_{a,1}\right) = A_c F_R \left[DNI\left(\tau\alpha\right) - U_{loss}\left(T_{abs} - T_a\right)\right]$	18
$T_{a,2} = T_{a,1} + \frac{A_c F_R \left[DNI\left(\tau\alpha\right) - U_{loss}\left(T_{abs} - T_a\right)\right]}{\dot{m}_a C_{pa}}$	19
$F_R = \frac{\dot{m}_a C_{pa}}{A_c U_{loss}} \left\{1 - \exp\left[\frac{U_{loss} F A_c}{\dot{m}_a C_{pa}}\right]\right\}$	20
$\dot{m}_{sw} h_{sw3} + \dot{m}_a h_{a2} = \dot{m}_{bw} h_{bw4} + \dot{m}_a h_{a3}$	21
$\dot{m}_{bw} = \dot{m}_{sw} - \dot{m}_{fw}$	22
$\dot{m}_{cw}\left(h_{cw,o} - h_{cw,i}\right) + \dot{m}_{fw} h_{fw} = \dot{m}_a \left(h_{a3} - h_{a4}\right)$	23
$\dot{m}_{fw} = \dot{m}_{da}\left(\omega_{a3} - \omega_{a4}\right)$	24
$\dot{m}_{da} = \frac{\dot{m}_a}{\left(1 + \omega_{a2}\right)}$	25
$h_{a,i} = 1.006 T_{a,i} + \omega_{a,i}\left(2501 + 1.86 T_{a,i}\right)$	26
$h_{w,i} = d_1 + d_2 T_{w,i} + d_3 T_{w,i}^2 + d_4 T_{w,i}^3 + d_5 T_{w,i}^4 + d_6 T_{w,i}^5$	27
$\omega_{a,i} = \frac{0.622 \times P_{s,i}}{P_{air,i}} = \frac{0.622 \times P_{s,i}}{P_a - P_{s,i}}$	28
$P_{s,i} = \frac{RH_{a,i}}{T_{a,i}^{8.2}} \times \exp\left[\left(77.3450 + \left(0.005 T_{a,i}\right)\right) - \left(\frac{7235}{T_{a,i}}\right)\right]$	29
$P_m = 4 \times P_{m,STC}\left(\frac{DNI}{DNI_{STC}}\right)\left[1 - \alpha_p\left(T_c - T_{c,STC}\right)\right]$	30
$\dot{m}_{fw} = \dot{m}_{da}\left(\omega_{a3} - \omega_{a4}\right)$	31
$RR_{HDH} = \frac{\dot{m}_{fw}}{\dot{m}_{sw}}$	32

The variable used in the mathematical model is defined in the table below

Variable	Definition	Value / Unit
T_{bs}	Backside surface temperature of PV module	$^{\circ}C$
T_w	temperature of sea water inlet	$^{\circ}C$
T_a	Air temperature	$^{\circ}C$
h_{p1}	glass cover penalty factor	0.8772
h_T	the tedlarheat transfer coefficient from back surface to air	500 W/m^2k
U_{tT}	The coefficient of overall heat transfer from glass cover to glass plate of PV	W/m^2k
$(\alpha\tau)_{eff}$	solar transmittance-absorptanceproduct	
T_c	PV module cell temperature	$^{\circ}C$
τ_G	the PV module glass cover transmittivity	0.95
α_C	the solar cell absorptivity	0.9
α_T	Tedlar absorptivity	

β_C	the solar cell packing factor	0.83
η_C	Electrical efficiency of PV module	
U_T	The coefficient of conductive heat transfer from PV cells to waterflows through the glass plate	W/m^2k
η_o	the referencePV-module efficiency	15%
T_{sw1}	Sea water temperature before PV panels	$°C$
T_{sw2}	Sea water temperature after PV panels	$°C$
h_{p2}	the glass plate penalty factor	0.9841
U_L	The coefficient of overall heat transfer from the PV module to thesurrounding on the backside	W/m^2k
A_C	The area of PV panels	m^2
m	Water mass	Kg
C_p	The specific heat capacity	4.2 $kJ/kg°C$
U_{tw}	The coefficient of overall heat transfer from the front glass of the PV module to water	W/m^2k
U_b	The coefficient of overall heat transfer from water to the surrounding,	W/m^2k
hi	the heat transfer cofficient of insulation	5.8 W/m^2k
L_i	Insulation thickness	0.05 m
k_i	insulation thermal conductivity	0.035 W/m^2k
L_g	the PV module glass thickness	0.003 m
k_g	the glass thermal conductivity of PV module	1 W/mk
$\dot{Q}_u$	gained useful energy	W
$\dot{Q}_{loss}$	Energy loss	W
D_{abs}	absorber tube diameter	0.047 m
L	Length	1.8 m
N	number of tubes	14
a_{abs}	is the absorptivity of selective coating	-
τ_g	the PV module glass cover transmittivity	096
DNI	direct normal solar irradiance	w/ m^2
$T_{SW,3}$	The seawater temperature at the outlet from the tube number 3	$°C$
$T_{SW,2}$	The seawater temperature at the outlet from the tube number 3	$°C$
$\dot{m}_{sw}$	Mass flow rate of sea water	m/s^2
C_P .	The specific heat	1.005 $kJ/kg\,K$
D_{abs}	the diameter of absorber tube	0.047 m
h_{abs-g}	the coefficient of convective heat transfer between the absorber and outer glass tube	0001115 W/m^2K
σ	the Stefan Boltzmann constant	5.67x10^{-8} W/m^2K^4
ε_{abs}	e emissivity of the absorber tube;	
T_S	the sky temperature	℃
T_{abs}	The temperature absorber	℃
$\dot{Q}_{\text{total}}$	The total heat absorbed	W

$\dot{Q}_u$	Useful heat	W
$\dot{Q}_{lass}$	The energy loss	W
A_c	cross-sectional area of collector	m^2
F_R	heat removal factor	
α_p	The power temperature coefficient	-0.38 $\%/K$
$\dot{m}_a\ \tau_g$	is the transmissivity of outer glass tube	0.95
DNI	The direct normal solar radiation	W/m2
U_{loss}	total loss coefficient	4.3 W/m2k
T_{abs}	The temperature of the absorber tube	$°C$
T_a	Air temperature	$°C$
	mass flow rate of the air	Kg/s
C_{pa}	the specific heat of the air	1.005 kJ/kg-K
$\tau\alpha$	transmissivity-absorptivity product	
$T_{a,2}$	Air temperature in	$°C$
$T_{a,1}$	Air temperature out	$°C$
F	collector efficiency factor	0.984
$\dot{m}_{sw}$	Mass flow rate of seawater	Kg/s
$\dot{m}_a$	air mass flow rate	Kg/s
h_{sw}	enthalpy of seawater	kJ/kg
h_a	enthalpy of air	kJ/kg
$\dot{m}_{fw}$	mass flow rate of freshwater	Kg/s
$\dot{m}_{fw}$	Mass flow rate of freshwater	Kg/s
$\dot{m}_{da}$	The mass flow rate of dry air	Kg/s
ω_a	humidity ratio of moist air	-
$h_{w,i}$	The saturated liquid water specific enthalpy	J/kg
$h_{a,i}$	Air specific enthalpy	J/kg
$T_{w,i}$	The saturated liquid water temperature	$^{\circ}°C$
$\omega_{a,i}$	Specific humidity of air	g water / Kg air
d_1	Factor	– 2.844699 × 10-2
d_2	Factor	4.211925
d_3	Factor	– 1.017034 × 10-3
d_4	Factor	1.311054 × 10-5
d_5	Factor	– 6.756469 × 10-8
d_6	Factor	1.724481 × 10-10
$\omega_{a,i}$	Air humidity ratio	%
$P_{s,i}$	vapor pressure of air in stream i	kPa
P_a	total pressure of moist air	101.2 kPa
$P_{air,i}$	partial pressure of dry air	kPa
$P_{s,i}$	Vapor pressure of air out of PV gap	kPa
$T_{a,i}$	Temperature of air at PV gap	$°C$

$RH_{a,i}$	relative humidity of air	$\%$
P_m	The output power produced from each PVpanels	Watt
$P_{m,STC}$	The peak power at standard test condition	180 Watt
DNI	The direct normal solar radiation	W/m^2
DNI_{STC}	The direct normal solar radiation at standard test condition	$1000\,W/m^2$
α_p	The power temperature coefficient	$-0.38\,\%/K$
T_c	The cell temperature	$°C$
$T_{c,STC}$	The cell temperature at standard test condition	$25\ °C$
$\dot{m}_{fw}$	The mass flow rate of freshwater	kg/s
$\dot{m}_{da}$	The mass flow rate of dry air	kg/s
ω_{a3}	humidity ratio of moist air inflow	
ω_{a4}	humidity ratio of moist air outflow	
RR_{HDH}	The recovery ratio of the HDH desalination unit	
$\dot{m}_{fw}$	The mass flow rate of freshwater	kg/s
$\dot{m}_{sw}$	The massflow rate of feed seawater	kg/s

TABLE1: The definitions, values and unit of the variables used in the mathematical model.

6. RESULTS AND DISCUSSION

6.1 Solar Radiation and Weather of Tabuk

FIGURE2 represents the amount of solar irradiance, in W/m^2, incident on a horizontal surface in the Tabuk region of Saudi Arabia during the four seasons of the year: Winter, Spring, Summer, and Fall.In Winter, from 6:00 to 8:00 AM, the amount of solar irradiance is relatively low, ranging from 22.9 to 390.7 W/m². However, the irradiance increases as the day progresses, reaching a maximum value of 616.3 W/m² at 10:00 AM, before gradually decreasing again.In Spring, the amount of solar irradiance is generally higher than in Winter, with a peak value of 758.6 W/m² at 10:00 AM. The irradiance also follows a similar pattern as in Winter, increasing in the morning and decreasing in the afternoon.In Summer, the amount of solar irradiance is the highest of all the seasons, with a peak value of 735.8 W/m² at 10:00 AM. The irradiance is relatively constant throughout the day, with little variation between morning and afternoon.In Fall, the amount of solar irradiance is similar to that in Spring, with a peak value of 636.9 W/m² at 11:00 AM. However, the irradiance decreases more rapidly in the afternoon than in Spring.Overall, the data shows that the amount of solar irradiance in the Tabuk region of Saudi Arabia varies significantly throughout the day and between the different seasons. This information can be useful for planning solar energy projects and optimizing the design of solar panels for maximum efficiency.

Also, FIGURE2 shows the temperature in Celsius (°C) for each hour of the day in four seasons (Winter, Spring, Summer, and Fall) for Tabuk, Saudi Arabia. The winter season is characterized by low temperatures, with the average temperature ranging from 5.4°C at 4 am to 6.9°C at midnight. In Spring, the average temperature is moderate, ranging from 14.8°C at midnight to 30.1°C at 10 am. Summer is the hottest season, with the average temperature ranging from 24.4°C at midnight to 39.4°C at 1 pm. Finally, Fall is characterized by a moderate temperature, with the average temperature ranging from 12.9°C at 4 am to 26.7°C at 11 am.The data indicates a significant variation in temperature throughout the day and throughout the year. This variation is expected due to Tabuk's location in a desert region, which experiences high temperatures during the day and low temperatures at night. The high temperatures in summer can be attributed to the region's proximity to the equator and the prevalence of dry desert winds. The low temperatures in winter can be attributed to the region's distance from the equator and the prevalence of cold desert winds.

The wind speed data for Tabuk, Saudi Arabia shows that the highest wind speeds occur during the afternoon hours in the summer season, with an average of 3.8-4.4 km/h. During the winter and fall seasons, the wind speed is relatively low, with average speeds ranging from 2.9-3.6 km/h, as depicted in FIGURE2. It is important to note that wind speed can have a significant impact on the local weather conditions, such as affecting the rate of evaporation and the amount of moisture in the air. In the summer season, the higher wind speeds can help to alleviate the hot and humid conditions, while in the winter and fall seasons, the lower wind speeds may contribute to cooler temperatures and less moisture in the air.Overall, the wind speed data for Tabuk shows a consistent pattern throughout the year, with relatively low speeds during the winter and fall seasons and higher speeds during the summer season.

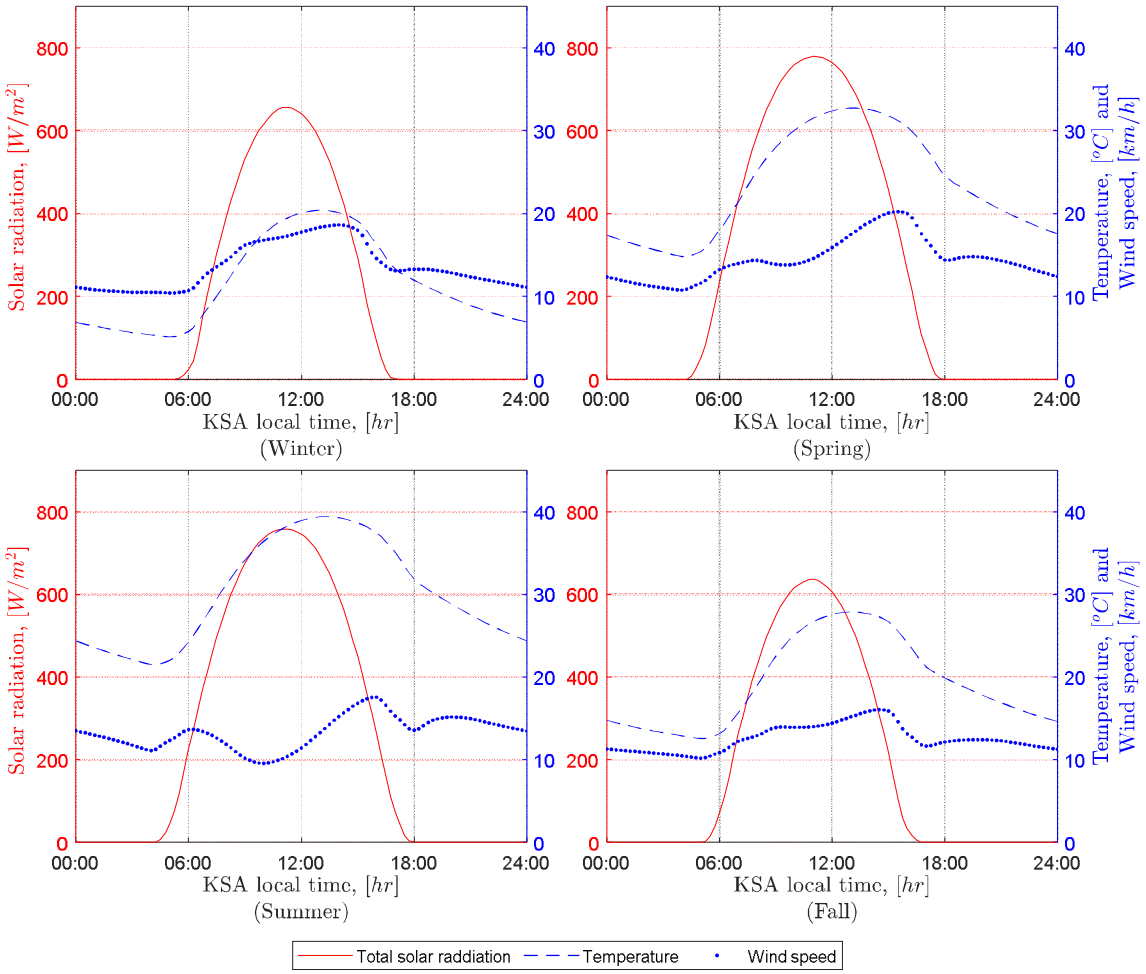

FIGURE2: Solar radiation on horizontal surface and weather conditions for Tabuk /KSA around the year.

FIGURE 3 regarding the total daily incident solar irradiance on the horizontal surface for the Tabuk region in KSA provides important information for understanding the availability of solar energy in the region. This information can be used to assess the feasibility of using solar energy for various applications, including HDH desalination.

It is noteworthy that the solar radiation in the Tabuk region is relatively high, especially in spring and summer seasons, which is common in many regions in the Middle East. This high solar radiation in the summer months can be leveraged to optimize the performance of solar-powered HDH systems and ensure that they are able to produce a sustainable supply of fresh water.

The daily incident solar irradiance on a horizontal surface ranges from 15.6 MW/m^2/day in fall to 23.1 MW/m^2/day in spring.During winter, the daily incident solar irradiance is 16.1 MW/m^2/day, which is lower than the values observed in spring and summer but higher than the value observed in fall. This indicates that winter in Tabuk receives a moderate amount of solar irradiance, which is still sufficient to influence the local climate.During spring, the daily incident solar irradiance is highest at 23.1 MW/m^2/day, which is significantly higher than the values observed in fall and winter. This indicates that spring in Tabuk is characterized by a high amount of solar irradiance, which contributes to the hot and arid climate of the region.During summer, the daily incident solar irradiance is 22.4 MW/m^2/day, which is slightly lower than the value observed in spring but significantly higher than the values observed in fall and winter. This indicates that summer in Tabuk is characterized by a high amount of solar irradiance, which contributes to the extremely hot and arid climate of the region.During fall, the daily incident solar irradiance is lowest at 15.6 MW/m^2/day, which is significantly lower than the values observed in spring and summer. This indicates that fall in Tabuk receives a relatively low amount of solar irradiance, which contributes to the cooler climate of the region during this season.However, it is also important to consider the variation in solar radiation throughout the year and to design the system to accommodate these fluctuations. The lower solar radiation in the winter and fall may require the use of energy storage systems or other measures to ensure that the HDH system can continue to operate even during periods of low solar radiation.

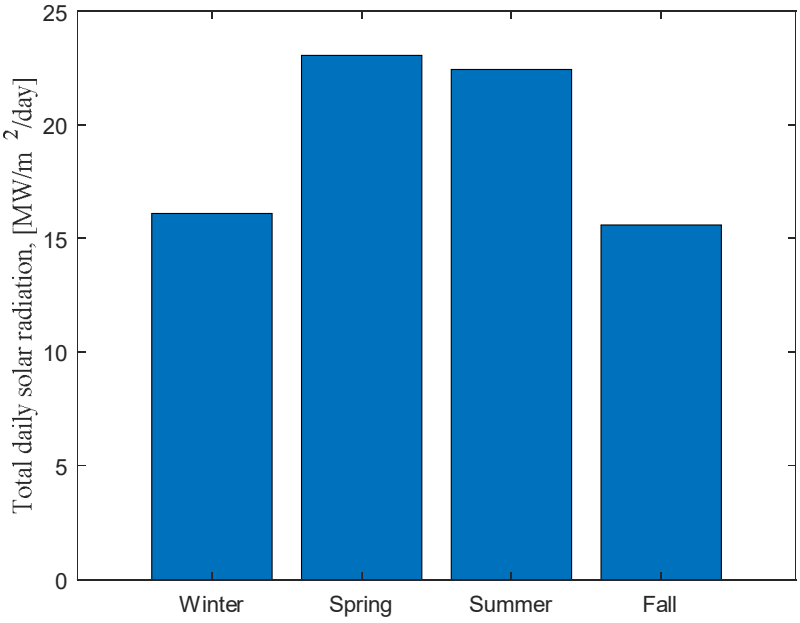

FIGURE 3: Total solar on horizontal surface radiation for Tabuk.

6.2 The Performance of Compact HDH Desalination System

FIGURE 4represents the numerical results of the mathematical model for a solar-powered HDH (humidifier dehumidification) desalination system, where the humidifier temperature is calculated in increments of 15 minutes over a 24-hour period. The results show that the temperature of the humidifier fluctuates throughout the day, with higher temperatures during peak solar hours (07:00am to 06:00pm) and lower temperatures at night when there is less sunlight.

The data provided represents the temperature of saline in a storage tank that is fed from a solar collector. The temperatures range from 28.2°C to 39.5°C throughout the year.During the winter season, the temperature of the saline in the tank ranges from 28.4°C to 33.1°C, with an average temperature of 30.3°C. In the spring season, the temperature ranges from 29.5°C to 39.2°C, with an average temperature of 34.5°C. In the summer season, the temperature ranges from 30.1°C

to 39.4°C, with an average temperature of 35.6°C. Finally, in the fall season, the temperature ranges from 29.1°C to 39.2°C, with an average temperature of 34.4°C.Overall, the temperature of the saline in the storage tank is highest in the summer season and lowest in the winter season, with a significant increase in temperature from winter to summer. This temperature difference reflects the availability of solar radiation and higher temperatures during summer months that allow for more efficient energy collection and storage. These high temperatures could be an advantage in HDH systems where a higher temperature difference between the hot and cold streams can increase the efficiency of the humidification process.

Based on the data provided in FIGURE 4, it can be observed that the temperature of the HDH humidifier is generally higher than the temperature of the saline in the storage tank fed from the solar collector. This is expected, as the HDH humidifier is designed to heat and humidify air using the hot saline solution from the storage tank.The temperature of the HDH humidifier shows a similar seasonal trend as the temperature of the saline in the storage tank, with higher temperatures observed in the summer months and lower temperatures in the winter months. However, the temperature difference between the seasons is not as significant as that observed in the saline temperatures.During the summer months, the temperature of the HDH humidifier is generally between 30-35°C, which is within the optimal temperature range for the humidification process. In contrast, during the winter months, the temperature of the HDH humidifier can drop to as low as 28°C, which may have a negative impact on the humidification process and overall system performance.

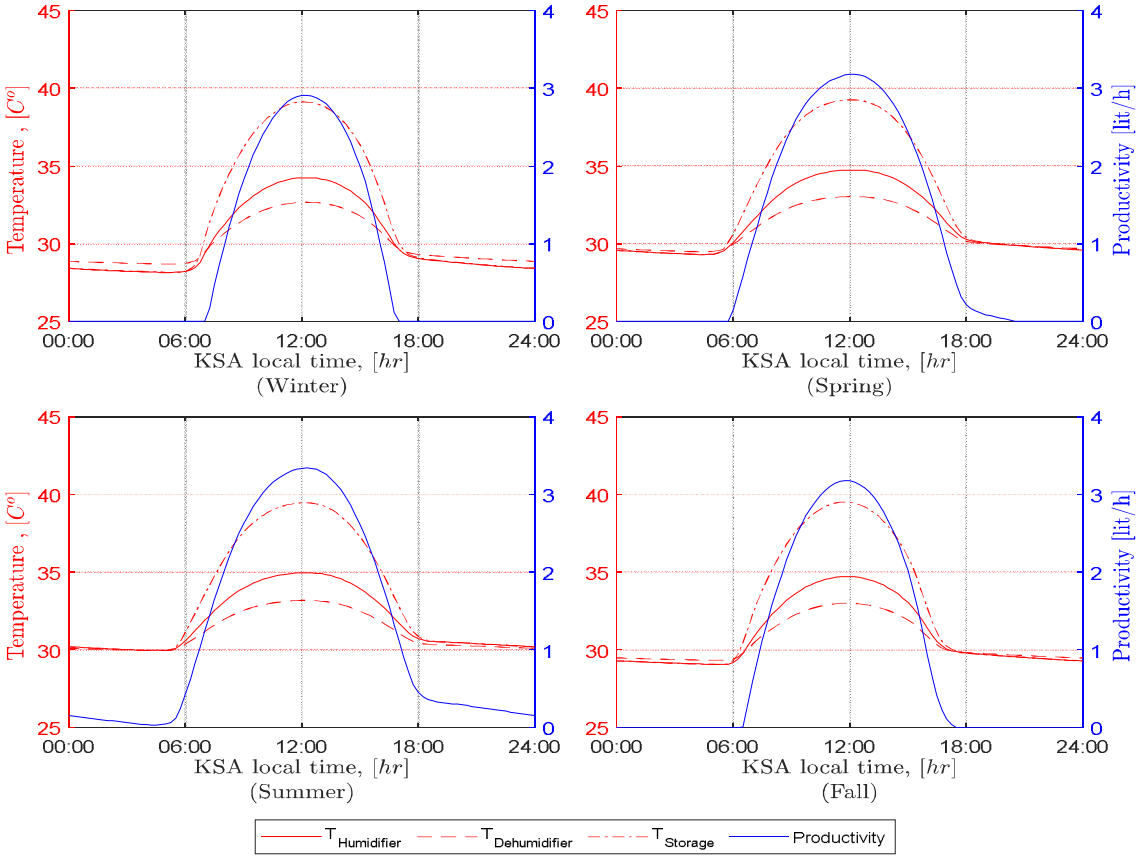

FIGURE 4: The performance of HDH desalination system under Tabuk solar and weather conditions.

From FIGURE 4, it appears that the temperatures of the HDH dehumidifier and humidifier both follow a similar trend throughout the year. In both cases, temperatures are highest during the summer months and lowest during the winter months. The difference in temperature between the

two is relatively small, with the dehumidifier being slightly cooler than the humidifier.In more detail, during the winter, the temperatures of the HDH humidifier and dehumidifier range from 28.4°C to 34.2°C and 28.7°C to 32.7°C, respectively. In the spring, temperatures range from 29.5°C to 34.7°C for the humidifier and 29.6°C to 32.2°C for the dehumidifier. During the summer months, the humidifier temperature ranges from 30.1°C to 34.9°C, while the dehumidifier temperature ranges from 30.0°C to 33.1°C. Finally, in the fall, the temperature range for the humidifier is 29.3°C to 34.5°C, while the dehumidifier ranges from 29.4°C to 32.9°C.It's worth noting that the specific temperatures for both the humidifier and dehumidifier will depend on various factors, including room temperature, humidity levels, and the specific model and settings of the device. Nonetheless, this data suggests that the temperature range of the HDH humidifier and dehumidifier can vary by a few degrees throughout the year, and that the temperature range for the humidifier is slightly wider than that of the dehumidifier.

The freshwater production from the HDH unit varies significantly across the different seasons of the year. In winter, the unit produces almost no fresh water, with a production rate of 0.00 lit/h. This is due to the low humidity levels in the cold winter air. In spring, the freshwater production increases to 0.80 lit/h at 7am and reaches a maximum production rate of 3.17 lit/h at 12pm. This increase is attributed to the rise in temperature and humidity levels. During summer, the freshwater production reaches its peak at 3.32 lit/h at 01:00 pm, which is the highest production rate throughout the year, indicating high humidity and temperature levels, as depicted in FIGURE 4. However, in fall, the freshwater production starts to decline, reaching a minimum of 0.22 lit/h at 5pm, due to the decrease in temperature and humidity levels.The highest production rates are observed during the midday hours, which is when the temperature and humidity levels are the highest, and they decline in the morning and evening hours, when the temperature and humidity are relatively low. It is important to note that the maximum production rate in summer is only about three times higher than the minimum production rate in winter, indicating that the HDH unit is not very efficient in producing freshwater during the cold winter months. The data suggests that the HDH unit can produce sufficient freshwater during the spring, summer, and early fall seasons, but additional water production methods might be necessary during the winter season.

Based on the provided data in FIGURE5, the seasonal production of freshwater is highest during the summer season, with 2786.1 lit/m^2/season. This is followed by the spring season with a production of 2226.9 lit/m^2/season, while the fall season has the lowest freshwater production of 1695.8 lit/m^2/season.The efficiency of the HDH unit also follows a similar trend, with the highest efficiency observed during the summer season at 41.2%. The spring season has the second-highest efficiency of 32.0%, followed by the fall season at 29.0%. The winter season has the lowest efficiency of 13.8%.It is interesting to note that the highest freshwater production and efficiency occur during the hottest season of the year (summer). This is likely due to the fact that the HDH unit operates by utilizing the temperature difference between the warm seawater and the cool air, and the greater the temperature difference, the more efficient the system is.On the other hand, the lower efficiency and freshwater production observed during the winter season could be due to the lower temperature difference between the seawater and air, resulting in reduced heat transfer and thus lower efficiency.Overall, the data suggests that the HDH unit is most effective during the summer season, which could have implications for the design and operation of such systems in different regions.

In this study, the HDH gain ratio during the summer season was determined to be approximately 0.4. It is worth noting that the reported gain ratios in other studies conducted by different authors exhibit significant variability.(Elzayed et al., 2021) reported a gain ratio of 0.99, indicating a high efficiency of the HDH system in their research. This suggests that their system achieved a nearly one-to-one ratio of freshwater production to solar energy input. (A. S. A. Mohamed et al., 2021) obtained a gain ratio of 0.81 in their study. Although slightly lower than the previous research, it still demonstrates a significant level of efficiency in freshwater production through the HDH system.These different gain ratios reflect the variations in system design, operating parameters, and environmental conditions in each study. It highlights the importance of considering these factors when evaluating the performance and efficiency of HDH systems.Further analysis and

comparison of these studies could provide valuable insights into optimizing HDH systems for efficient and sustainable freshwater production.

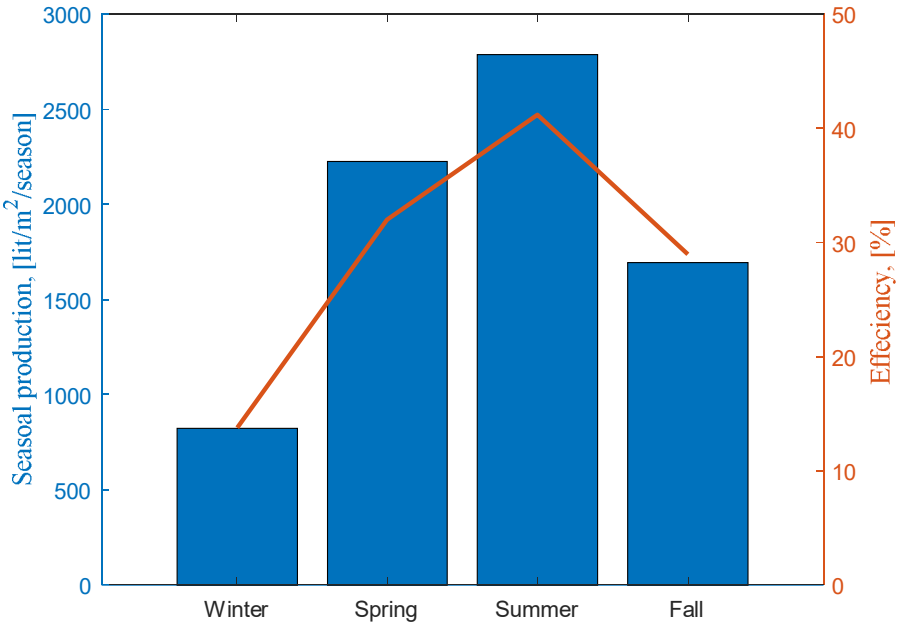

FIGURE5: Seasonal production of fresh water, and efficiency of HDH system under Tabuk solar and weather conditions.

The paper provides valuable insights into the use of a compact and domestic air humidification dehumidification (HDH) desalination system, which is suitable for remote areas with limited water resources and experienced operators. The study presents a mathematical model to analyze the impact of various operating parameters on the system's productivity. The paper suggests that the use of a solar-powered HDH desalination system can be a potential solution to address the scarcity of sustainable and renewable sources of water in Saudi Arabia. The study also emphasizes the importance of considering the variation in solar radiation throughout the year and designing the system to accommodate these fluctuations. The paper provides a mathematical model that can be used to optimize the performance of solar-powered HDH systems and ensure that they are able to produce a sustainable supply of fresh water. Overall, the paper contributes to the development of more efficient and sustainable desalination systems that can be used in remote areas with limited water resources.

The results suggest that the use of a solar-powered HDH desalination system can be a potential solution to address the scarcity of sustainable and renewable sources of water in Saudi Arabia. The study also emphasizes the importance of considering the variation in solar radiation throughout the year and designing the system to accommodate these fluctuations. Overall, the paper contributes to the development of more efficient and sustainable desalination systems that can be used in remote areas with limited water resources.

7. CONCLUSION

The data presented in the article provides important information about the solar irradiance, temperature, and wind speed in the Tabuk region of Saudi Arabia. The amount of solar irradiance varies significantly throughout the day and between the different seasons, with the highest irradiance occurring in the summer season. The temperature in Tabuk also varies significantly throughout the day and throughout the year, with the hottest temperatures occurring in summer and the coldest temperatures occurring in winter. Wind speed is relatively low during the winter and fall seasons and higher during the summer season.

The daily incident solar irradiance on a horizontal surface ranges from 15.6 MW/m^2/day in fall to 23.1 MW/m^2/day in spring, with winter receiving a moderate amount of solar irradiance. The high solar radiation in the summer months can be leveraged to optimize the performance of solar-powered HDH systems and ensure that they are able to produce a sustainable supply of fresh water. The data can be useful for planning solar energy projects and optimizing the design of solar panels for maximum efficiency.

The results suggest that Tabuk has a high potential for solar energy production, particularly in the summer season. The information provided in the article can be used to assess the feasibility of using solar energy for various applications, including HDH desalination, and to inform the design of solar energy systems.

The results indicate that the HDH unit is most effective in producing freshwater during the summer season, with the highest freshwater production rate of 2786.1 lit/m2/season and the highest efficiency of 41.2%. This is followed by the spring season, which has a freshwater production rate of 2226.9 lit/m2/season and an efficiency of 32.0%. The fall season has the lowest freshwater production rate of 1695.8 lit/m2/season and an efficiency of 29.0%, while the winter season has the lowest efficiency of 13.8%.

The higher freshwater production and efficiency observed during the summer season is likely due to the greater temperature difference between the warm seawater and cool air, resulting in more efficient heat transfer. In contrast, the lower temperature difference during the winter season may lead to reduced heat transfer, resulting in lower efficiency and freshwater production. Therefore, the data suggests that the HDH unit should be designed and operated with the summer season in mind to ensure the highest efficiency and freshwater production rates.

It should be noted that there could be various factors affecting the efficiency of the HDH unit, such as weather conditions and maintenance. Therefore, further analysis and evaluation of the data may be needed to determine the most optimal conditions for maximizing the freshwater production and efficiency of the HDH unit.

8. CONFLICTS OF INTEREST

The authors declare that they have no known competing financial interests or personal relationships that could have appeared to influence the work reported in this paper.

9. DATA AVAILABILITY

The data that support the findings of this study are available from the corresponding author upon reasonable request.

10. REFERENCES

Abdel Dayem, A. M., & AlZahrani, A. (2022). Psychometric study and performance investigation of an efficient evaporative solar HDH water desalination system. *Sustainable Energy Technologies and Assessments*, *52*(PA), 102030. https://doi.org/10.1016/j.seta.2022.102030

Abdullah, A. S., Omara, Z. M., Essa, F. A., Alarjani, A., Mansir, I. B., & Amro, M. I. (2021). Enhancing the solar still performance using reflectors and sliding-wick belt. *Solar Energy*, *214*(December 2020), 268–279. https://doi.org/10.1016/j.solener.2020.11.016

Abu Mallouh, M., AbdelMeguid, H., & Salah, M. (2022). A comprehensive comparison and control for different solar water heating system configurations. *Engineering Science and Technology, an International Journal*, *35*(2022), 101210. https://doi.org/10.1016/j.jestch.2022.101210

Aburub, A., Aliyu, M., Lawal, D., & Antar, M. A. (2017). Experimental Investigations of a Cross-Flow Humidification Dehumidification Desalination System. *International Water Technology*, *7*(3), 198–208.

Ahmed, M. M. Z., Alshammari, F., Abdullah, A. S., & Elashmawy, M. (2021). Experimental investigation of a low cost inclined wick solar still with forced continuous flow. *Renewable Energy*, *179*, 319–326. https://doi.org/10.1016/j.renene.2021.07.059

Criscuoli, A., & Carnevale, M. C. (2022). Localized Heating to Improve the Thermal Efficiency of Membrane Distillation Systems. In *Energies* (Vol. 15, Issue 16). MDPI. https://doi.org/10.3390/en15165990

El-Ghetany, H. H., & Khattab, N. M. (2016). Mathematical modeling for performance prediction of a humidification - dehumidification solar water desalination system in Egypt. *Egyptian Journal of Chemistry*, *59*(2), 145–162. https://doi.org/10.21608/ejchem.2016.937

El-Sharkawy, I. I., Abdelmeguid, H., & Saha, B. B. (2013). Towards an optimal performance of adsorption chillers: Reallocation of adsorption/desorption cycle times. *International Journal of Heat and Mass Transfer*, *63*(0), 171–182. https://doi.org/10.1016/j.ijheatmasstransfer.2013.03.076

El-Sharkawy, Ibrahim I., AbdelMeguid, H., & Saha, B. B. (2014). Potential application of solar powered adsorption cooling systems in the Middle East. *Applied Energy*, *126*(0), 235–245. https://doi.org/10.1016/j.apenergy.2014.03.092

El-Sharkawy, Ibrahim I, Abdelmaguid, H., Saha, B. B., Koyama, S., & Miyazaki, T. (2013). Performance Investigation of A Solar-Powered Adsorption Cooling System: A Case Study for Egypt. In *International Symposium on Innovative Materials for Processes in Energy Systems 2013 (IMPRES2013)*.

Elsharkawy, M., AbdelMeguid, H., El-Sharkawy, I. I., & Rabie, L. (2014). Experimental and theoretical investigation of decentralized desalination system. *Mansoura Engineering Journal*, *39*(2).

Elzayed, M. S., Ahmed, M. A. M., Antar, M. A., Sharqawy, M. H., & Zubair, S. M. (2021). The impact of thermodynamic balancing on the performance of a humidification dehumidification desalination system. *Thermal Science and Engineering Progress*, *21*. https://doi.org/10.1016/j.tsep.2020.100794

Fares, M. N., Al-Mayyahi, M. A., Rida, M. M., & Najim, S. E. (2019). Water Desalination Using a New Humidification-Dehumidification (HDH) Technology. *Journal of Physics: Conference Series*, *1279*(1). https://doi.org/10.1088/1742-6596/1279/1/012052

Farmani, R, Butler, D., Memon, F., Abdelmeguid, H., & Ward, S. (2011). Sustainable water management for urban regeneration. In *The Future of Urban Water: Solutions for Livable and Resilient Cities*.

Farmani, Raziyeh, Butler, D., Hunt, D. V. L., Memon, F. A., Abdelmeguid, H., Ward, S., & Rogers, C. D. F. (2012). Scenario-based sustainable water management and urban regeneration. *Proceedings of the Institution of Civil Engineers: Engineering Sustainability*, *165*(1), 89–98. https://doi.org/10.1680/ensu.2012.165.1.89

Kabeel, A. E., Diab, M. R., Elazab, M. A., & El-Said, E. M. S. (2022a). Hybrid solar powered desalination system based on air humidification dehumidification integrated with novel distiller: Exergoeconomic analysis. *Journal of Cleaner Production*, *379*(P1), 134690. https://doi.org/10.1016/j.jclepro.2022.134690

Kabeel, A. E., Diab, M. R., Elazab, M. A., & El-Said, E. M. S. (2022b). Solar powered hybrid desalination system using a novel evaporative humidification tower: Experimental investigation. *Solar Energy Materials and Solar Cells*, *248*(September), 112012. https://doi.org/10.1016/j.solmat.2022.112012

Kabeel, A. E., Hamed, M. H., Omara, Z. M., & Sharshir, S. W. (2013). Water Desalination Using a Humidification-Dehumidification Technique—A Detailed Review. *Natural Resources*, *04*(03), 286–305. https://doi.org/10.4236/nr.2013.43036

Khalaf-Allah, R. A., Abdelaziz, G. B., Kandel, M. G., & Easa, A. S. (2022). Development of a centrifugal sprayer-based solar HDH desalination unit with a variety of sprinkler rotational speeds and droplet slot distributions. *Renewable Energy*, *190*, 1041–1054. https://doi.org/10.1016/j.renene.2022.04.019

Manju, S., & Sagar, N. (2017). Renewable energy integrated desalination: A sustainable solution to overcome future fresh-water scarcity in India. *Renewable and Sustainable Energy Reviews*, *73*(February), 594–609. https://doi.org/10.1016/j.rser.2017.01.164

Memon, F. A., Butler, D., Farmani, R., Abdelmeguid, H., Atkinson, S., Rogers, C., & Hunt, D. (2011). Urban Futures – Sustainability (Resilience) Evaluation of Water Infrastructure . In *The 2011 AEESP Education & Research Conference*.

Mohaisen, H. S., Esfahani, J. A., & Ayani, M. B. (2021). Improvement in the performance and cost of passive solar stills using a finned-wall/built-in condenser: An experimental study. *Renewable Energy*, *168*, 170–180. https://doi.org/10.1016/j.renene.2020.12.056

Mohamed, A. M. I., & Elminshawy, N. A. S. (2009). Humidification-dehumidification desalination system driven by geothermal energy. *Desalination*, *249*(2), 602–608. https://doi.org/10.1016/j.desal.2008.12.053

Mohamed, A. S. A., Shahdy, A. G., & Salem Ahmed, M. (2021). Investigation on solar humidification dehumidification water desalination system using a closed-air cycle. *Applied Thermal Engineering*, *188*. https://doi.org/10.1016/j.applthermaleng.2021.116621

Moumouh, J., Tahiri, M., & Balli, L. (2018). Solar Desalination by Humidification-Dehumidification of Air. *MATEC Web of Conferences*, *149*, 1–4. https://doi.org/10.1051/matecconf/201714902092

Nakamura, A., Ota, Y., Koike, K., Hidaka, Y., Nishioka, K., Sugiyama, M., & Fujii, K. (2015). A 24.4% solar to hydrogen energy conversion efficiency by combining concentrator photovoltaic modules and electrochemical cells. *Applied Physics Express*, *8*(10). https://doi.org/10.7567/APEX.8.107101

Prakash, A., & Jayaprakash, R. (2021). Performance evaluation of stepped multiple basin pyramid solar still. *Materials Today: Proceedings*, *45*, 1950–1956. https://doi.org/10.1016/j.matpr.2020.09.227

Sayed, E. T., Olabi, A. G., Elsaid, K., Al Radi, M., Alqadi, R., & Ali Abdelkareem, M. (2022). Recent progress in renewable energy based-desalination in the Middle East and North Africa MENA region. *Journal of Advanced Research*, *48*, 125–156. https://doi.org/10.1016/j.jare.2022.08.016

Shafieian, A., Rizwan Azhar, M., Khiadani, M., & Kanti Sen, T. (2020a). Performance improvement of thermal-driven membrane-based solar desalination systems using nanofluid in the feed stream. *Sustainable Energy Technologies and Assessments*, *39*(February). https://doi.org/10.1016/j.seta.2020.100715

Shafieian, A., Rizwan Azhar, M., Khiadani, M., & Kanti Sen, T. (2020b). Performance improvement of thermal-driven membrane-based solar desalination systems using nanofluid in the feed stream. *Sustainable Energy Technologies and Assessments*, *39*. https://doi.org/10.1016/j.seta.2020.100715

Sukpancharoen, S., & Phetyim, N. (2021). Green hydrogen and electrical power production through the integration of CO2 capturing from biogas: Process optimization and dynamic control.

Energy Reports, *7*, 293–307. https://doi.org/10.1016/j.egyr.2021.06.048

Tahir, F., & Al-Ghamdi, S. G. (2022). Integrated MED and HDH desalination systems for an energy-efficient zero liquid discharge (ZLD) system. *Energy Reports*, *8*, 29–34. https://doi.org/10.1016/j.egyr.2022.01.028

Ward, S., Abdelmeguid, H., Farmani, R., Memon, F. A., & Butler, D. (2011). Sustainable water management - Modelling acceptability for decision support: A methodology. In *Urban Water Management: Challenges and Oppurtunities - 11th International Conference on Computing and Control for the Water Industry, CCWI 2011* (Vol. 1).

Zaragoza, G., Ruiz-Aguirre, A., & Guillén-Burrieza, E. (2014). Efficiency in the use of solar thermal energy of small membrane desalination systems for decentralized water production. *Applied Energy*, *130*, 491–499. https://doi.org/10.1016/j.apenergy.2014.02.024.